**Differential regulation of TROP2 release by PKC isoforms through vesicles and ADAM17**

Tim M. Wanger[ǂ], Sharon Dewitt[ǂ], Anne Collins[√], Norman J. Maitland[√], Zaruhi Poghosyan[≠] and Vera Knäuper [ǂǁ]

[ǂ]College of Biomedical and Life Sciences, Cardiff University, Dental School, Cardiff, CF14 4XY, United Kingdom.
[√]YCR Cancer Research Unit, Department of Biology, University of York, York, YO10 5DD, United Kingdom.
[≠]College of Biomedical and Life Sciences, Cardiff University, Medical School, Cardiff, CF14 4XN, United Kingdom.

**Running title:** Regulation of TROP2 release by PKCs

**Keywords:**
TROP2, PKC, ectodomain shedding, microvesicles, ADAM17

**Abstract**

TROP2, a cancer cell surface protein with both pro-oncogenic and anti-oncogenic properties is cleaved by ADAM17. ADAM17 dependent cleavage requires novel PKC activity which is blocked by the ADAM10/ADAM17 inhibitor GW64 as well as by the PKC inhibitor Bim-1. Full length TROP2 release is induced by classical PKC activation and blocked by Gö6979, without affecting ADAM17 dependent TROP2 cleavage. Full length TROP2 is released in ectosomes, as inhibition of endocytosis did not prevent release. Inhibition of the atypical PKC isoform PKCζ stimulated metalloproteinase dependent N-terminal alternative TROP2 cleavage. The resulting alternative TROP2 cleavage product remains membrane associated via a disulphide bond, but is released in microvesicles with an average size of 107 nm. Inhibition of endocytosis following PKCζ inhibition prevented alternative cleavage and release of TROP2, suggesting that these events require endocytic uptake and exosomal release of the corresponding microvesicles. The alternative TROP2 cleavage product was also found in PC3 cell lysates following deglycosylation, and may represent a novel biomarker in prostate cancer.

## 1. Introduction

TROP2, an epithelial cancer marker, that also defines prostate stem cells [1] is overexpressed in many cancers, where high expression levels often correlate with poor prognosis/survival [2-6]. Recent contradicting literature evidence suggests that TROP2 expression, as well as cellular localisation and proteolysis status, determines patient survival rates and outcome [6-10]. In lung cancer, membrane associated TROP2 binds IGF1 via the EGF-like and the thyroglobulin (TY)-domain and here TROP2 acts as a tumour suppressor [9] and is epigenetically silenced. In breast cancer, the subcellular localisation of TROP2 at the cell membrane predicts worse survival, compared to cases showing intracellular staining for immature, non glycosylated TROP2, predicting increased survival [10]. Similarly, novel Fab-TROP2 antibodies inhibit breast cancer growth *in vitro* and *vivo* [11]. TROP2 recruits neuregulin-1 in the cytosolic compartment, which required both EGF-like and TY-TROP2 domains in some head and neck squamous cell carcinomas (HNSCC). TROP2 loss in HNSCC increased neuregulin-1 cell surface levels and neuregulin-1 shedding. The increased neuregulin-1 shedding leads to ErbB3 activation, driving tumour progression, with subsequent ErbB3 antibody therapy arresting tumour growth [8]. In prostate cancer, TROP2 is cleaved by ADAM17 and γ-secretase and nuclear intracellular TROP2 (TROP2-ICD) forms a complex with β-catenin. This supports cancer stem cell self-renewal and hyperplasia *in vivo*, indicating a link between TROP2 signalling and the wnt pathway [7]. Furthermore, overexpression of the TROP2-ICD promoted hyperplasia and upregulated cyclinD1 and c-myc expression [7]. However, the molecular mechanism by which shedding of TROP2 is regulated has not been studied in detail.

One of the major pathways regulating ectodomain shedding of ADAM17 substrates involves the activation of PKC family members [12]. PKCδ and PKCα were previously reported to regulate HB-EGF release [13-15]; PKCδ and PKCη were shown to be involved in IL-6 receptor cleavage [16]. PKCε was associated with TNFα shedding [17], whereas PKCδ [18] and PKCζ regulate NRG processing [15, 19]. It is possible that regulation of shedding by PKC isoforms does not occur through modulation of ADAM activity, but through modification of substrates or substrate-selecting factors [20] (reviewed in [21]). Indeed, it was shown for the NRG precursor that its cytoplasmic tail is required for ADAM17 mediated ectodomain shedding [22], which required substrate phosphorylation on S386, as a prerequisite for induced shedding [15, 19]. In addition, inhibition of PKCζ using a myristoylated pseudosubstrate peptide inhibitor enhanced NRG release in response to PMA stimulation (Dang et al. 2011).

Alternative pathways to generate soluble membrane proteins involve the formation of membrane microvesicles or exosomes. This allows the exchange of growth factor receptors, growth factor ligands as well as proteolytic enzymes amongst others between tumour cells and/or stromal cells (reviewed in [23-25]). For example increasing evidence shows that exosomes produced by fibroblasts

or macrophages can influence tumourigenesis both by promoting [26] or inhibiting cancer progression [27]. Cancer cells also release numerous factors in microvesicles or exosomes which increase survival signalling and prevent cell death as exemplified by exosomal TNFR1 preventing cell death signalling [28]. On the other hand, tumour exosomes can induce stromal exosome release, promoting a tumour niche containing fractalkine ligand (CX3CL1) that then activates chemokine receptor CXCR1 signalling in the tumour [29]. These mechanisms can work in concert with ectodomain shedding. For example γ-radiation, doxorubicin treatment or oncogene induced tumour cell senescence, caused ADAM17 dependent proteolytic release of soluble TNFR1-ECD and amphiregulin-ECD, which was accompanied by full length ICAM1 release in exosomes [30].

The regulation of TROP2 cleavage by ADAM17 had not been investigated in detail and we here set out to analyse the contribution of different PKC isoforms in regulating TROP2 release and cleavage. We present new evidence showing differential regulation of full length TROP2 release in vesicles and regulated intramembrane proteolysis in response to PKC activation. In contrast, PKCζ inhibition activates a distinct pathway, producing an alternative N-terminal TROP2 cleavage product, which remains membrane associated via an internal disulphide bridge, but is released in exosomal vesicles into the extracellular space.

## 2. Materials and methods

### *2.1 Chemicals and antibodies*

R&D systems supplied goat anti-hTROP2 antibody (AF650) and Invitrogen mouse anti-V5 antibody (R-96025). Rabbit anti-PKC-ζ (9372S) and and mouse anti-HA (H6908) were from New England Biolabs. Secondary antibodies conjugated to HRP were from Jackson Immunoresearch, and Alexa dye secondary antibody conjugates were from Invitrogen/Molecular probes. The cell impermeable PKC-ζ pseudopeptide (PS) and cell permeable myristoylated pseudosubstrate (mPS) peptides with the sequence SIYRRGARRWRKL and Myr-SIYRRGARRWRKL were purchased from R&D systems. The myristoylated control peptide with a scrambled sequence of Myr-SRIYRGRARWRLK (scrambled mPS) was custom synthesized by GeneScript. Chemicals were from Sigma unless stated otherwise. Restriction enzymes were from Promega and cell culture medium from Gibco. The ADAM inhibitors GI23 and GW64 were a kind gift from Dr. Augustin Amour at GlaxoSmithKline.

### *2.2 TROP2 expression constructs and cell lines:*

Full-length TROP2 was amplified using Phusion DNA polymerase (Thermo Scientific) with the forward primer and reverse PCR primer:

5’-AAAGCTAGCATGGCTCGGGGCCCCGGCCTCGCGCCG-3’ (For)

5’-AAACTCGAGCAAGCTCGGTTCCTTTCTCAACTCCCCC-3’ (Rev) in HF buffer supplemented with DMSO. The PCR product was cleaved with NheI and XhoI and ligated into pcDNA5/V5/His, thereby introducing a C-terminal V5/His tag. An N-terminal heamagglutinin and alkaline phosphatase

tagged TROP2 (AP-TROP2) construct was generated using the following primer: 5'AAAAGATCTCAGGACAACTGCACGTGTCCCACCAAC3' and the reverse primer from above and are schematically shown in Figure S1D. The resulting PCR product was cleaved with BglII and XhoI prior to ligation into AP-pcDNA5/V5/His [31]. All expression constructs were sequenced and were error free. Stable cell lines were established using the Invitrogen Flp-In system according to the manufacturer's instructions.

***2.3 Analysis of PKC dependent release of Alkaline Phosphatase (AP)-tagged TROP2 (AP-TROP2) into medium:***

The AP-TROP2-expressing HEK293 cell line was used to analyse AP activity in medium as described [31] using 24 well plates and 4 replicas for each condition. PMA was used at 100 ng/ml in serum free Optimem medium to activate classical and novel PKCs. Time course experiments established an optimal time point of 3h to assess AP-TROP2 release. Metalloproteinase inhibitor experiments were performed using 1 µM GI23 or GW64 to selectively inhibit ADAM10 or ADAM17, respectively, by incubating cells over night with inhibitor prior to PMA stimulation in their presence or absence. Some experiments were performed in the presence of the classical or novel PKC inhibitors Gö6979 or Bim-1 using 1h pre-incubation at 1 µM inhibitor concentrations followed by 3h PMA stimulation in the presence or absence of these inhibitors. Additional experiments were performed using the myristoylated pseudosubstrate (mPS) PKCζ inhibitor or appropriate peptide controls, lacking myristoylation (PS) or a scrambled myristoylated control peptide (scrambled PS). Cells were incubated with 10 µM mPS, scrambled PS or PS for up to 3h and AP-activity analysed in medium. Metalloproteinase or PKC inhibitor experiments were performed as described for PMA. The involvement of dynamin dependent endocytosis was analysed using dynasore at 80 µM concentrations and a 30 min preincubation period. Cells were then treated for 3h with PMA or mPS in the presence or absence of dynasore.

2.4 ***AP-TROP2 release in response to knockdown of PKCζ using shRNA targeting plasmids***

The following shRNA expression plasmids were from Sigma-Aldrich (MISSION shRNA) and used to ablate PKCζ expression.

PKCζ:

CCGGCGCGTGATTGACCCTTTAACTCTCGAGAGTTAAAGGGTCAATCACGCGTTTTT

Control:

CCGGGCGCGATAGCGCTAATAATTTCTCGAGAAATTATTAGCGCTATCGCGCTTTTT

Briefly, HEK293 cells were seeded at 0.5 x $10^5$ cells/well on polylysine-coated 24-well plates and grown overnight. 6 µl of FuGENE 6 transfection reagent was diluted in 400 µl of serum-free medium prior to the addition of 1µg shRNA expression plasmid and 1µg AP-TROP2 expression plasmid and incubated for 20 min. 100µl of the shRNA/AP-TROP2 transfection mixtures was then pipetted into each well. The transfected cells were cultured for 48h. The medium was removed, the cell monolayer washed with serum free Optimem prior to addition of 250 µls Optimem for 3h and analysis of

medium AP-activity. Western blot analysis of lysates was performed to assess even transfection efficiency for TROP2 expression levels across experiments and also analysed for PKCζ expression levels and include a GAPDH loading control.

***2.5 Analysis of full length and cleaved TROP2 in medium:***

The medium from TROP2 release experiments was centrifuged for 10 min at room temperature (20°C) and 13.000 rpm to pellet dead cells and cell debris, and concentrated using Amicon Ultra-4 centrifugal concentration tubes with a 11kDa molecular mass cut-off. The final concentrate was diluted with 2x Laemmli sample buffer under reducing or non-reducing conditions, denatured at 95°C for 3 min and analysed by SDS-PAGE and Western Blotting.

To separate microvesicles and soluble AP-TROP2 the cleared medium was subjected to ultracentrifugation at 100000g for 1h at 4°C using a Sorvall discovery 100SE ultracentrifuge equipped with T-1250 rotor. The resulting pellet was dissolved in 2x Laemmli sample buffer using reducing or non-reducing conditions. The supernatant from the ultracentrifugation experiment was concentrated using Amicon Ultra-4 centrifugal concentration tubes prior to SDS-PAGE and Western blotting.

***2.6 Analysis of TROP2 fragments in cell lysates and medium by SDS-PAGE and Western blotting:***

Medium was removed from cells and used for shedding assays or ultracentrifugation experiments whilst the remaining cell monolayer was washed with PBS and lysed in 20mM sodium phosphate, pH 7.4, 150 mM NaCl, 1% Triton X-100 supplemented with proteinase inhibitor mixture (Roche), 10mM 1,10-phenantroline and 250µg/ml sodium vanadate. The lysates were centrifuged to remove cell debris and protein content was determined using the DC protein assay (Bio-Rad) prior to equal loading of lysates. Tricine-SDS-PAGE was conducted according to the method by [32] and proteins transferred to PVDF membranes. Proteins were detected using primary antibodies (1:2000) with appropriate secondary antibodies conjugated to horseradish peroxidase (1:10000) allowing visualization using enhanced chemiluminescence. Equal loading was verified using a mouse monoclonal GAPDH antibody (Sigma at 1:2000). Western blots from lysates derived from PMA stimulation experiments were quantified using a BIO-RAD imaging system and band volumes quantified using Image Lab Software version 5.1. The density of the MP-band in a lane was divided by the density of the GAPDH loading control. The data was then normalised to the DMSO solvent control and expressed as fold changes in a bar diagram summarising three blots from independent experiments.

***2.7 Nanoparticle tracking analysis (NTA):***

Real time detection, counting and sizing of extracellular vesicles released into medium was performed using a Nanosight LM10 instrument (NanoSight Ltd. UK), consisting of a conventional optical microscope, charge-coupled device camera and a LM10 sample unit with a laser light source. Conditioned media was taken off the cells and centrifuged for 10 min at 13.000 rpm in order to remove intact cells and debris. Approximately 300 µl of the samples were injected into the LM10 unit with a 1ml sterile syringe. Capturing settings were manually set for optimal detection according to the

manufacturer's protocols (shutter: 9ms; gain: 250). The LM10 was used to record 60 second sample videos which were than analysed with the Nanoparticle Tracking Analysis (NTA) 2.0 analytical software. Appropriate control measurements were performed with medium supplemented with reagents used to evaluate vesicle release. The calculated concentration values as well as the size distribution tables were then exported and further analysed in GraphPad Prism®.

***2.8 Confocal analysis of TROP2 expression levels and cellular localization:***

HEK293 cells stably expressing AP-TROP2 were seeded onto poly-L-lysine coated glass cover slips in 24-well plates at a cell density of 0.2 x $10^5$ cells/well. They were cultured for 48 h in DMEM/10% FBS and then stimulated using various conditions as outlined above prior to immunodetection of AP-TROP2. Cells were washed with PBS, fixed with 4% paraformaldehyde in PBS for 7 min and then washed three times with PBS. They were then permeabilised with 0.5% saponin/PBS for 10 min, washed three times with PBS and blocked for 30 min in 1% BSA/PBS blocking buffer. Subsequently, the cells were incubated with both mouse anti-V5 (1:500) and goat anti-TROP2 (1:500) primary antibodies in blocking buffer at 4°C for 2h in a humidified chamber. Cells were then washed three times with PBS, incubated with both anti-mouse AlexaFluor®594 and anti-goat AlexaFluor®488 secondary antibodies in blocking buffer for 1h at room temperature. Surplus antibody was removed by washing three times with PBS. Nuclei were counter stained with DAPI-containing vectashield mounting medium (Vector Laboratories). Slides were analysed using a Leica SP5 confocal microscope (Leica, Microsystems) and images acquired with a 63× oil immersion objective with NA = 1.4 (HCX PF APO CS 63.0X1.40 OIL UV) using sequential scanning at 488 and 543 nm. A 10µm size bar is shown in all images. TROP2-ICD staining is shown in red and TROP2-ECD staining in green. Co-localisation analysis was performed using ImageJ, JACoP plugin and the Pearson's coefficient determined from the green and red channels respectively. R values above 0.75 were considered a good indication of co-localisation. Mean fluorescence intensity of membrane staining was quantified using ImageJ.

***2.9 Statistical data analysis:***

Data presented are from three independent shedding experiments with 4 internal replicas per experimental condition. AP-substrate hydrolysis rates were calculated and data normalized by dividing data from treated samples with the control data of the appropriate solvent control. Data are mean +/- S.D. and were analyzed with GraphPad Prism using One-way Anova with Tukey post-test. P values below 0.05 were considered significant.

Lysates derived from shedding experiments were combined from 4 wells to generate sufficient lysates for analysis. Equal protein concentrations were loaded and analyzed using Tris/Tricine SDS-Page and

transferred to PVDF membranes. Normalized data from three Western blots are shown for PMA stimulation as indicated in 2.6. Bar graphs presented are mean +/- S.E.M. and were analyzed with GraphPad Prism using repeated analysis One-way Anova with Tukey post-test. P values below 0.05 were considered significant.

## 3. Results

### *3.1 Regulation of TROP2 shedding by classical and novel PKC activation leads to full length TROP2 release and ADAM17 dependent shedding*

To further investigate the role of PKCs in regulating TROP2 cleavage by ADAMs we created an AP-TROP2 expression construct and tested whether Ionomycin or PMA were able to induce TROP2 cleavage. Fig. 1A shows that PMA induced TROP2 shedding which additionally led to an accumulation of an 11 kDa metalloproteinase fragment in cell lysates (Fig. 1B). Western blot analysis of the medium in non-reducing conditions showed an increase in full length TROP2 in PMA stimulated conditions detected with anti-V5 antibody and the presence of TROP2-ECD dimers and monomers in the medium when stained with anti-TROP2 antibody (Fig. 1C). The data indicated that TROP2 is not only cleaved, but also released as a full length molecule into the extracellular environment. Inhibition experiments with GW64 and GI23 ADAM inhibitors revealed partial inhibition of TROP2 release by GW64, an inhibitor preferentially blocking ADAM17 activity (Fig. 1D). GW64 also partially blocked the production of the 11 kDa MP-fragment in cell lysates (Fig. 1E and Fig. S1A for quantification of three blots) and TROP2-ECD release into medium (Fig. 1F), confirming a previous report that TROP2 shedding is mediated by ADAM17 [7]. Ultracentrifugation experiments were performed with conditioned medium from shedding experiments to verify the nature of the V5 positive TROP2 species and showed that the pellet obtained at 100000xg contained the full length protein, as well as a novel, alternative cleavage product of 45 kDa (aMP), staining positive for the C-terminal V5 epitope (Fig. 1G). In contrast, soluble TROP2-ECD dimers and monomers were enriched in the soluble fraction (Fig. S1 B).

### *3.2 Classical PKC activation promotes full length AP-TROP2 release in microvesicles while novel PKC activation induces ADAM17 dependent AP-TROP2 cleavage*

Having established that TROP2 release was a combination of full length release and proteolytic cleavage we next wanted to establish whether these events were differentially regulated by different PKC isoforms. We employed the well characterised PKC inhibitors Gö6979 and Bim-1 to evaluate the role of classical and novel PKC isoforms in promoting full length TROP2 release versus proteolytic cleavage. Inhibition of classical PKCs with Gö6979 partially blocked the release of AP-activity, while Bim-1 completely inhibited PMA stimulated release (Fig. 2A). Gö6979 blocked only full length AP-TROP2 release, with AP-TROP2-ECD signals still up regulated in medium when compared to DMSO control (Fig. 2B). This was accompanied with an increase in 11 kDa MP fragment intensities in lysates treated with PMA and Gö6979 when compared to Gö6979 solvent control (Fig. 2C/D), although changes were low following quantification and statistically not significant. In contrast, Bim-1 dependent inhibition of classical and novel PKC isoforms, prevented ~~both cleavage and~~ full length AP-TROP2 release into medium (Fig. 2A, B) and ~~also~~ prevented

increases in MP-fragment formation in response to PMA stimulation (Fig. 2C, Bim-1 panel). However, the densities of the 11 kDa MP fragment showed small increases, which may reflect changes in fragment turnover when novel and classical PKCs are blocked pharmacologically. Since full length membrane proteins can be released via vesicles we next analysed particle release using a Nanosight instrument. This analysis demonstrated that PMA treatment triggered vesicle release, and confirmed that inhibition of classical PKCs was sufficient to ablate vesicle formation (Fig. 2E, Gö6979 panel). The vesicle size ranges from 50 to 250 nm (Fig. 2F) and thus they could represent exosomes or ectosomes [33].

### *3.3 Inhibition of endocytosis leads to loss of cell surface AP-TROP2 and partial intracellular accumulation of perinuclear TROP2-ICD in control and PMA stimulated conditions*

We next wanted to establish whether inhibition of endocytosis using dynasore would effect vesicle or cleavage dependent TROP2 release. In the presence of dynasore, TROP2 levels in medium increased 4 fold regardless of PKC activation status (Fig. 3A), but the 11 kDa MP-fragment levels only increased in PMA treated samples when compared to controls (Fig. 3B). Medium analysis demonstrated a dramatic increase in full length TROP2 release in dynasore treated conditions (Fig. 3C) and virtually complete loss of cell surface TROP2 staining as assessed by confocal microscopy (Fig. 3D, anti TROP2 panel, green, Dynasore panel -/+ PMA). Controls showed good co-localisation between TROP2-ECD (green) and the V5-tag at C-terminus (red), with a Pearson's coefficient of 0.79. Some loss of co-localisation occurred in PMA stimulated conditions, leading to partial perinuclear localisation of C-terminal TROP2 fragment(s), but co-localisation at the membrane was not significantly effected (Fig. 3D, merged arrow, red, PMA control, Pearson's coefficient r=0.77). Partial perinuclear C-terminal V5-tag TROP2 staining was also apparent in dynasore treated samples (Fig. 3D, dynasore panels, red, arrows). Upon dynasore and PMA co-treatment we observed also some membrane staining for the TROP2-MP fragment retaining the V5-epitope tag (Fig. 3C, dynasore + PMA panel, red, bold arrows). These data were confirmed by fluorescence intensity analysis of membrane staining for TROP2-ECD and –ICD, demonstrating an increase in TROP2-ICD staining in PMA/dynasore co-treated samples (Fig. 3E). Therefore our data indicate that full length vesicular TROP2 undergoes rapid endocytosis and when endocytosis is blocked the vesicles containing TROP2 accumulate in the environment.

### *3.4 Loss of PKCζ activity leads to alternative TROP2 cleavage*

To establish the role of atypical PKCs in TROP2 shedding, we next employed a myristoylated pseudosubstrate (mPS) to inhibit PKCζ [15] and determined the release rate of AP-TROP2 into the medium. Figure 4A shows that mPS treatment resulted in a decrease of AP-TROP2 in medium at 30 min, while at 120 min mPS treatment caused significantly elevated AP-TROP2 levels in the medium

when compared to the solvent control. A representative Western blot for this time course is shown in Fig. S1C which demonstrates the production of an alternative 45 kDa fragment at the 30 min time point which increases in intensity over time. Since mPS can cause unspecific side effects [34, 35], we compared its effect to those of the pseudosubstrate peptide lacking the N-terminal myristoylation (PS) and a scrambled myristoylated control peptide (scrambled mPS). Treatment with mPS showed a dramatic increase in TROP2 release into medium, relative to control and PS treated cells. There was some increase in shedding in the scrambled mPS control peptide treated sample (Fig. 4B). Western blot analysis revealed a significant increase in the aMP fragment running at 45 kDa in the cell lysate (Fig. 4C, mPS lane) without causing an increase in the 11 kDa MP fragment. Additionally we detected an alternative ECD fragment in cell lysates under reducing conditions using the TROP2 and HA antibodies that recognises N-terminal TROP2 (Fig. 4D). These data indicate that alternative cleavage occurs at the EGF-like and TY-domain intersection and these fragments remain associated via a disulphide bond and cannot be distinguished from full length AP-TROP2 in non-reducing conditions. We next co-transfected cells with PKCζ shRNA or control shRNA, to confirm that the mPS result was indeed due to inhibition of PKCζ. PKCζ was significantly reduced upon shPKCζ treatment, when compared to shRNA control treatment (Fig. 4E). This resulted in a significant increase in TROP2 release into medium (Fig. 4F), and correlated with an increase in the 45 kDa aMP fragment in lysates which was quantified using densitometry over the GAPDH loading control and required long blot exposure times to obtain significant amounts of 45 kDa fragment in sh-control treated samples (Fig. 4G). To validate that alternatively cleaved AP-TROP2 does not solely release the HA-AP-tag we also investigated TROP2-V5 expressing cells (Fig. S1D schematic representation of expression constructs) by treating them with mPS. Lysates from AP-TROP2 and TROP2-V5 cells were deglycosylated with PNGaseF and fragment sizes compared by Western blotting. Fig. S2A and S2B show that aMP cleavage is induced by mPS treatment and the fragment size was identical after deglycosylation and showed a molecular mass of 32 kDa. This confirms our assessment that alternative cleavage occurs at the EGF-TY-domain interface. We also noted that LNCaP cells were negative for aMP TROP2 fragments, whilst PC3 cells were positive, indicating that alternative cleavage occurs in more aggressive prostate cancer cells (Fig. S2C & D).

### *3.5 Alternative TROP2 cleavage is metalloproteinase dependent, independent of classical or novel PKC activity and involves release in vesicles*

We next wanted to investigate whether alternative cleavage of AP-TROP2 required metalloproteinase activity. AP-TROP2 release was investigated after treating cells with the ADAM10/ADAM17 inhibitor GW64, the ADAM10 inhibitor GI23 and the general metalloproteinase inhibitor GM6001. Fig. 5A shows that GW64 and GM6001 were most effective at preventing mPS induced AP-TROP2 release into medium, which was confirmed by Western blot analysis of cell lysates for the 45 kDa

aMP (Fig. 5B). In contrast ADAM10 inhibition was less effective, although some inhibition was seen in both AP-assays and Western blot analysis of the aMP fragment. The data indicate that ADAM17 is the main protease responsible for alternative TROP2 cleavage. We next tested whether classical or novel PKC activity was involved in alternative TROP2 cleavage. Inhibition of classical and novel PKCs with Gö6979 and Bim-1 did not affect the mPS induced release of AP-TROP2 into medium (Fig. 5C) and did not inhibit the formation of the 45 kDa aMP fragment (Fig. 5D). We next wanted to establish whether mPS dependent AP-TROP2 release was associated with changes in vesicle number or size released from our cells. Fig. 5E shows a particle size analysis using Nanosight, demonstrating that mPS treatment led to an increase in particle numbers with slightly reduced size. However the increase in particle numbers was not significantly larger than the solvent control vesicle numbers (Fig. 5F).

### *3.6 AP-TROP2 release in response to PKCζ inhibition and alternative cleavage requires endocytosis*

When we investigated the time course of mPS induced AP-TROP2 release we noted that there was a significant loss of TROP2 in the medium at the 30 min time point which potentially indicated that TROP2 was initially undergoing endocytosis, followed by its subsequent release. We therefore tested whether TROP2 release in response to loss of PKCζ activity was dependent on endocytosis using dynasore treatment (Fig. 6A). The experiment showed that mPS dependent AP-TROP2 release is blocked by dynasore treatment. This is in complete contradiction with PMA induced vesicle release and shedding (Fig. 3) which showed accumulation in medium in the presence of dynasore. Therefore TROP2 release due to loss of PKCζ activity requires endocytosis suggesting these are exosomes. This was confirmed by analysing particle size as well as release using the Nanosight instrument. mPS treated samples contained smaller vesicles and additionally their numbers were significantly decreased in the presence of dynasore (Fig. 6 B&C). Western blot analysis of cell lysates confirmed that aMP fragment formation was impaired in the presence of dynasore (Fig. 6D). In medium, dynasore and mPS cotreated samples showed loss of the AP-TROP2 band running at 130 kDa in non-reducing conditions (Fig. 6E, left panel, 130 kDa band, dynasore + mPS), which corresponded with the loss of the aMP fragment containing the V5 epitope tag in reducing conditions (Fig. 6E, right panel, lack of 45 kDa aMP band in the dynasore + mPS lane). Confocal analysis of TROP2-ECD and –ICD domains showed good co-localisation in both control and mPS treated conditions (Fig. 6F, DMSO control -/+ mPS; Pearson's coefficient 0.82 and 0.84). In dynasore treated conditions there was loss of TROP2-ECD staining in the control (Fig. 6F, dynasore – mPS; Pearson's coefficient 0.58), but not in mPS cotreated samples, where both TROP2-ECD and –ICD domains showed intense cell membrane staining (Fig. 6F, dynasore + mPS; Pearson's coeffient r=0.83). Fluorescence intensity analysis of confocal images confirmed that mPS treatment in the presence of dynasore preserved

membrane TROP2-ECD and –ICD staining (Fig. 6G), confirming the AP-TROP2 release and vesicle release data shown in Fig. 6A-6E.

## 4. Discussion

We here describe novel mechanisms regulating TROP2 release into the extracellular environment. Unlike a previous report focussing solely on ADAM17 dependent TROP2 cleavage resulting in the generation of TROP2-ECD and ICD fragments [7], we have identified additional mechanisms resulting in full length ectosomal, as well as exosomal release of alternatively cleaved membrane associated TROP2 from the cell surface. We noted that PMA stimulation of TROP2 release into the medium was only partially inhibited by the ADAM10/17 inhibitor GW64, indicating that other mechanisms of TROP2 release must exist (summarised in Fig. 7 A). The discovery of full length TROP2 in medium suggested that this might be due to vesicles budding from the cell surface, also called ectosomes. Ultracentrifugation studies showed that full length TROP2 was enriched in the insoluble pellet, while cleaved TROP2-ECD dimers were enriched in the medium fraction. The two events were distinguished using PKC inhibitors where loss of classical PKC activity specifically blocked full length TROP2 release in ectosomes. Additional inhibition of novel PKCs also inhibited the ADAM17 dependent cleavage of TROP2. We excluded that PMA induced vesicle dependent release of full length TROP2 was due to exosome formation. Dynasore treatment resulted in the accumulation of vesicles in the medium as assessed by both vesicle numbers and accumulation of full length TROP2 in medium. Thus PMA dependent TROP2 release is a combination of vesicle release and ADAM17 dependent shedding. Our observations may explain some of the recent contrasting observations on the TROP2 signalling potential as an oncogenic or anti-oncogenic cancer marker [1, 7-10, 36]. ADAM17 dependent TROP2-ECD and –ICD fragments independently promote prostate cancer hyperplasia, with TROP2-ICD binding β-catenin leading to up regulation of cyclin D1 and c-myc expression [7], indicating that TROP2 cleavage products have oncogenic potential. In contrast, full length TROP2 modulates IGF1-R signalling by sequestering IGF1 via EGF-TY domain interactions, leading to down regulation of proliferation in lung adenocarcinoma in response to IGF1 [9]. Therefore ectosomal full length TROP2 could conceivably behave like an IGF1 decoy receptor in lung cancer.

Secondly we identified a third pathway for TROP2 release in our model system where either inhibition or knockdown of PKCζ enriched an alternative TROP2 cleavage product, which required metalloproteinase activity and endocytic uptake of TROP2 (Summary Fig. 7B). We excluded that other PKC isoforms were involved in this process using pharmacological inhibitors. Our data suggest that cleavage occurs at the EGF-TY domain interphase, with fragments remaining connected via a disulphide bond as recently seen for the TROP2 homologue EpCAM [37]. The alternative TROP2

fragments remain attached to the cell membrane but are released in exosomal vesicles, as ultracentrifugation of the medium enriched the TROP2 fragments in the pellet fraction. Here the additional inhibition of endocytosis upon loss of PKCζ activity showed, that TROP2 release and cleavage at the alternative site were efficiently blocked, suggesting these events occur inside the cells. Therefore we conclude that loss of PKCζ activity leads to exosomal release of TROP2 fragments into the extracellular environment. We found a similar fragment in aggressive PC3 prostate cancer cell lysates but not in LNCaP lysates (Fig. S2 C&D), indicating that this occurs in aggressive prostate tumour cells. Furthermore loss of PKCζ leads to prostate cancer, where c-myc expression is upregulated [38], which could be potentially linked to TROP2 signalling. Additionally TROP2 expression is upregulated in prostate cancer stem cell lysates when compared to benign hyperplastic cell lysate which was negative (Fig. S2E). The molecular mass of TROP2 in these patient samples were below the expected size of fully glycosylated protein, however due to lack of sample size we could not deglycosylate the protein to investigate whether these bands were due to alternative TROP2 cleavage. It is currently unclear whether alternatively cleaved TROP2 has a specific function in prostate cancer or other malignancies. Conceivably the interaction between TROP2 and IGF1 could be compromised due to the cleavage of the protein at the EGF-TY domain interface, potentially ablating the tumour suppressive activity observed in lung cancer [9]. Furthermore, the recent finding that TROP2 regulates neuregulin cell surface levels is intriguing [8] and potentially linked to loss of PKCζ activity, as this induces endocytic uptake of TROP2 seen here. Additionally neuregulin shedding in response to PMA is enhanced following PKCζ inhibition [19]. Also PKCζ was recently shown to regulate Notch receptor routing [39]. These data indicate a regulatory role for PKCζ in regulating membrane localisation or exosomal TROP2 release, potentially dictating downstream signalling outcome.

Although exosomal release of the TROP2 homologue EpCAM from ovarian and breast tumour cells has been shown, the signalling mechanism regulating release has remained unexplored [40, 41]. Our data therefore represent the first evidence that PKC signalling is a major regulator of ectosomal and exosomal TROP2 release as well as proteolytic cleavage through ADAM17. Additionally we presented evidence of intracellular TROP2 processing by ADAM10 and ADAM17 at a novel N-terminal cleavage site at the EGF-TY domain interface. The identification of these separate pathways gives novel insights into mechanisms leading to TROP2 release relevant in cancer progression.

**Acknowledgements**

The Financial support of Tenovus (PhD2011/L25) to V. K. and Cancer Research Wales to Z. P. is gratefully acknowledged. We also thank Dr. Augustin Amour and GlaxoSmithKline for ADAM inhibitors. This paper is dedicated in loving memory to Charlotte and Helmut Knäuper.

References


[1] A. S. Goldstein, D. A. Lawson, D. Cheng, W. Sun, I. P. Garraway, O. N. Witte, *Proc. Natl. Acad. Sci. U. S. A* **2008**, *105*, 20882.

[2] E. Guerra, M. Trerotola, A. L. Aloisi, R. Tripaldi, G. Vacca, S. R. La, R. Lattanzio, M. Piantelli, S. Alberti, *Oncogene* **2013**, *32*, 1594.

[3] T. Liu, Y. Liu, X. Bao, J. Tian, Y. Liu, X. Yang, *PLoS. One.* **2013**, *8*, e75864.

[4] S. Ning, N. Liang, B. Liu, X. Chen, Q. Pang, T. Xin, *Neurol. Sci.* **2013**, *34*, 1745.

[5] X. Liu, S. Li, F. Yi, *J. Cancer Res. Clin. Oncol.* **2014**.

[6] M. Trerotola, P. Cantanelli, E. Guerra, R. Tripaldi, A. L. Aloisi, V. Bonasera, R. Lattanzio, L. R. de, U. H. Weidle, M. Piantelli, S. Alberti, *Oncogene* **2013**, *32*, 222.

[7] T. Stoyanova, A. S. Goldstein, H. Cai, J. M. Drake, J. Huang, O. N. Witte, *Genes Dev.* **2012**, *26*, 2271.

[8] K. Zhang, L. Jones, S. Lim, C. A. Maher, D. Adkins, J. Lewis, R. J. Kimple, E. J. Fertig, C. H. Chung, A. Herrlich, M. J. Ellis, B. A. Van Tine, L. S. Michel, *Oncotarget.* **2014**.

[9] J. C. Lin, Y. Y. Wu, J. Y. Wu, T. C. Lin, C. T. Wu, Y. L. Chang, Y. S. Jou, T. M. Hong, P. C. Yang, *EMBO Mol. Med.* **2012**, *4*, 472.

[10] F. Ambrogi, M. Fornili, P. Boracchi, M. Trerotola, V. Relli, P. Simeone, S. R. La, R. Lattanzio, P. Querzoli, M. Pedriali, M. Piantelli, E. Biganzoli, S. Alberti, *PLoS. One.* **2014**, *9*, e96993.

[11] H. Lin, H. Zhang, J. Wang, M. Lu, F. Zheng, C. Wang, X. Tang, N. Xu, R. Chen, D. Zhang, P. Zhao, J. Zhu, Y. Mao, Z. Feng, *Int. J. Cancer* **2014**, *134*, 1239.

[12] K. Horiuchi, G. S. Le, M. Schulte, T. Yamaguchi, K. Reiss, G. Murphy, Y. Toyama, D. Hartmann, P. Saftig, C. P. Blobel, *Mol. Biol. Cell* **2007**, *18*, 176.

[13] Y. Izumi, M. Hirata, H. Hasuwa, R. Iwamoto, T. Umata, K. Miyado, Y. Tamai, T. Kurisaki, A. Sehara-Fujisawa, S. Ohno, E. Mekada, *EMBO J.* **1998**, *17*, 7260.

[14] M. Kveiborg, R. Instrell, C. Rowlands, M. Howell, P. J. Parker, *PLoS. One.* **2011**, *6*, e17168.

[15] M. Dang, K. Dubbin, A. D'Aiello, M. Hartmann, H. Lodish, A. Herrlich, *J. Biol. Chem.* **2011**, *286*, 17704.

[16] W. Thabard, M. Collette, R. Bataille, M. Amiot, *Biochem. J.* **2001**, *358*, 193.

[17] D. L. Wheeler, K. J. Ness, T. D. Oberley, A. K. Verma, *Cancer Res.* **2003**, *63*, 6547.

[18] R. M. Esper, J. A. Loeb, *J. Biol. Chem.* **2009**, *284*, 26251.

[19] M. Dang, N. Armbruster, M. A. Miller, E. Cermeno, M. Hartmann, G. W. Bell, D. E. Root, D. A. Lauffenburger, H. F. Lodish, A. Herrlich, *Proc. Natl. Acad. Sci. U. S. A* **2013**, *110*, 9776.

[20] T. Maretzky, D. R. McIlwain, P. D. Issuree, X. Li, J. Malapeira, S. Amin, P. A. Lang, T. W. Mak, C. P. Blobel, *Proc. Natl. Acad. Sci. U. S. A* **2013**, *110*, 11433.

[21] M. Hartmann, A. Herrlich, P. Herrlich, *Trends Biochem. Sci.* **2013**, *38*, 111.

[22] X. Liu, H. Hwang, L. Cao, D. Wen, N. Liu, R. M. Graham, M. Zhou, *J. Biol. Chem.* **1998**, *273*, 34335.

[23] T. H. Lee, E. D'Asti, N. Magnus, K. Al-Nedawi, B. Meehan, J. Rak, *Semin. Immunopathol.* **2011**, *33*, 455.

[24] M. Shimoda, R. Khokha, *Proteomics.* **2013**, *13*, 1624.

[25] V. Muralidharan-Chari, J. W. Clancy, A. Sedgwick, C. D'Souza-Schorey, *J. Cell Sci.* **2010**, *123*, 1603.

[26] M. Shimoda, S. Principe, H. W. Jackson, V. Luga, H. Fang, S. D. Molyneux, Y. W. Shao, A. Aiken, P. D. Waterhouse, C. Karamboulas, F. M. Hess, T. Ohtsuka, Y. Okada, L. Ailles, A. Ludwig, J. L. Wrana, T. Kislinger, R. Khokha, *Nat. Cell Biol.* **2014**, *16*, 889.

[27] H. D. Lee, B. H. Koo, Y. H. Kim, O. H. Jeon, D. S. Kim, *FASEB J.* **2012**, *26*, 3084.

[28] F. I. Hawari, F. N. Rouhani, X. Cui, Z. X. Yu, C. Buckley, M. Kaler, S. J. Levine, *Proc. Natl. Acad. Sci. U. S. A* **2004**, *101*, 1297.

[29] D. Castellana, F. Zobairi, M. C. Martinez, M. A. Panaro, V. Mitolo, J. M. Freyssinet, C. Kunzelmann, *Cancer Res.* **2009**, *69*, 785.

[30] T. Effenberger, H. J. von der, K. Bartsch, C. Garbers, K. Schulze-Osthoff, A. Chalaris, G. Murphy, S. Rose-John, B. Rabe, *FASEB J.* **2014**, *28*, 4847.

[31] N. Ali, V. Knauper, *J. Biol. Chem.* **2007**, *282*, 37378.

[32] H. Schagger, *Nat. Protoc.* **2006**, *1*, 16.

[33] E. Cocucci, G. Racchetti, J. Meldolesi, *Trends Cell Biol.* **2009**, *19*, 43.

[34] K. Krotova, H. Hu, S. L. Xia, L. Belayev, J. M. Patel, E. R. Block, S. Zharikov, *Br. J. Pharmacol.* **2006**, *148*, 732.

[35] S. Lim, J. W. Choi, H. S. Kim, Y. H. Kim, K. Yea, K. Heo, J. H. Kim, S. H. Kim, M. Song, J. I. Kim, S. H. Ryu, P. G. Suh, *Life Sci.* **2008**, *82*, 733.

[36] J. Wang, K. Zhang, D. Grabowska, A. Li, Y. Dong, R. Day, P. Humphrey, J. Lewis, R. D. Kladney, J. M. Arbeit, J. D. Weber, C. H. Chung, L. S. Michel, *Mol. Cancer Res.* **2011**, *9*, 1686.

[37] U. Schnell, J. Kuipers, B. N. Giepmans, *Biosci. Rep.* **2013**, *33*, e00030.

[38] J. Y. Kim, T. Valencia, S. Abu-Baker, J. Linares, S. J. Lee, T. Yajima, J. Chen, A. Eroshkin, E. A. Castilla, L. M. Brill, M. Medvedovic, M. Leitges, J. Moscat, M. T. Diaz-Meco, *Proc. Natl. Acad. Sci. U. S. A* **2013**, *110*, 6418.

[39] M. Sjoqvist, D. Antfolk, S. Ferraris, V. Rraklli, C. Haga, C. Antila, A. Mutvei, S. Y. Imanishi, J. Holmberg, S. Jin, J. E. Eriksson, U. Lendahl, C. Sahlgren, *Cell Res.* **2014**, *24*, 433.

[40] S. Runz, S. Keller, C. Rupp, A. Stoeck, Y. Issa, D. Koensgen, A. Mustea, J. Sehouli, G. Kristiansen, P. Altevogt, *Gynecol. Oncol.* **2007**, *107*, 563.

[41] A. K. Rupp, C. Rupp, S. Keller, J. C. Brase, R. Ehehalt, M. Fogel, G. Moldenhauer, F. Marme, H. Sultmann, P. Altevogt, *Gynecol. Oncol.* **2011**, *122*, 437.

**FIGURE CAPTIONS:**

**Figure 1: PMA stimulates full length TROP2 release as well as ADAM17 dependent TROP2 cleavage**

**(A)** TROP2 release into medium was stimulated by PMA but not Ionomycin. **(B)** PMA induces the production of a 11 kDa metalloproteinase fragment. Schematic representation of the AP-TROP2 expression construct, containing N-terminal HA and AP-tags as well as a C-terminal V5/His epitope tag. **(C)** Analysis of medium under non-reducing conditions revealed an increase in V5-positive full length AP-TROP2 in medium as well as AP-TROP2-ECD dimers and monomers in response to PMA stimulation (anti-TROP2 panel). **(D)** Inhibition of ADAM17 activity with GW64 partially inhibits PMA induced AP-TROP2 release, while ADAM10 inhibition has no effect. **(E)** Western blot analysis of lysates confirms that the 11 kDa fragment is the product of ADAM17 dependent AP-TROP2 cleavage. For quantification see Figure S1A. **(F)** Western blot analysis of medium in reducing conditions shows a reduction in AP-TROP2-ECD levels in GW64 treated samples, but not in GI23 treated samples when compared to DMSO solvent control. **(G)** Full length TROP2 in medium is found in the pellet fraction following ultracentrifugation of the medium. An alternatively cleaved V5-epitope positive TROP2 fragment running at 45 kDa was present.

**Figure 2: Full length AP-TROP2 is released in vesicles and requires classical PKC activity, while AP-TROP2 cleavage requires novel PKC activation**

**(A)** PMA induced AP-TROP2 release is partially blocked by inhibiting classical PKC activity with Gö6979 and completely with Bim-1 which inhibits both classical and novel PKC activity. **(B)** Gö6979 blocks full length AP-TROP2 release into medium, which Bim-1 prevents full length as well as AP-TROP2-ECD release. **(C)** Western blot analysis of lysates shows that Bim-1 prevents upregulation of the 11 kDa MP-fragment in response to PMA stimulation. (**D**) Quantification of 11 kDa MP fragment from AP-TROP2 shedding experiments shown in (A). Data are normalised to DMSO solvent control and mean +/-S.E.M. is represented. N=3 blots. **(E)** PMA induces particle release in AP-TROP2 expressing cells which is inhibited by Gö6979 and Bim-1. **(F)** PMA induced vesicles are approximately 50-250 nm in size.

**Figure 3: Inhibition of endocytosis with dynasore leads to loss of cell surface AP-TROP2 expression and partial accumulation of TROP2-ICD fragments in intracellular, perinuclear vesicles**

**(A)** Dynasore treatment lead to 4 fold increases in AP-TROP2 release into medium regardless of PMA treatment. **(B)** Dynasore treatment does not influence the generation of the 11 kDa MP-fragment in lysates. **(C)** Western blot analysis of medium in non-reducing and reducing conditions shows a

large increase of full length AP-TROP2. Under reducing conditions an additional V5-positive fragment is apparent. **(D)** Confocal analysis of TROP2-ECD and TROP2–ICD domains using anti-TROP2 (green) and anti-V5 (red) antibodies shows partial co-localisation in control and PMA stimulated conditions, with membrane and perinuclear TROP2-ICD staining more apparent after PMA stimulation (arrow overlay image + PMA). Dynasore treatment led to a dramatic loss of TROP2-ECD staining regardless of PMA co-treatment. TROP2-ICD was found at the cell membrane (bold arrows) and well as in the perinuclear region (arrows, dynasore +/- PMA panels), although membrane retained TROP2-ICD was more prominent in dynasore and PMA co-treated cells. Pearson's coefficient values were calculated as r=0.79, 0.77, 0.56 and 0.64 for each experimental condition. Bar is equivalent to 10 µm. **(E)** Fluorescence intensity analysis for TROP2-ECD and –ICD staining shows loss of cell surface fluorescence for DMSO or PMA treated samples in the presence of dynasore.

**Figure 4: Loss of PKCζ activity leads to alternative TROP2 cleavage**

**(A)** Time course of AP-TROP2 release into medium in response to treatment with a PKCζ myristoylated pseudosubstrate (mPS). AP-TROP2 levels in medium decreased at the 30 min time point while they significantly increased at 2h treatment when compared to solvent control. **(B)** Comparison of PS, scrambled mPS and mPS treatment to evaluate whether the observed increase in AP-TROP2 in medium was specific to PKCζ inhibition by mPS. Some non-specific side effects of scrambled mPS were seen. The experiment was terminated after 3h incubation with peptides. **(C)** Western blot analysis of cell lysates from the experiment shown in (B) using reducing conditions stained for the V5-epitope tag reveals a novel aMP fragment of 45 kDa in size in response to mPS treatment. The alternative cleavage site is indicated in the diagram. **(D)** Western blot analysis of cell lysates in reducing conditions comparing control and mPS stimulation stained with TROP2 antibody detects the aMP fragment and an additional novel aECD fragment (left panel). In contrast, staining with anti-HA antibody only recognises the aECD fragment (right panel). **(E)** Western blot analysis of PKCζ expression following PKCζ knockdown compared to a scrambled control shRNA. **(F)** Comparison of AP-TROP2 release between shRNA control and shPKCζ treatment shows a significant increase in AP-activity in medium upon PKCζ knockdown. **(G)** Quantification of the aMP fragment production in response to shPKCζ treatment over GAPDH loading control shows a significant increase in samples lacking PKCζ protein. Results are from three independent experiments performed with four internal repeats.

**Figure 5: Alternative TROP2 cleavage requires metalloproteinase activity and is independent of classical or novel PKC activity**

**(A)** Metalloproteinase inhibitors block mPS induced AP-TROP2 release into medium. Both ADAM17 (1 µM GW64) and ADAM10 (1 µM GI23) inhibition as well as 25 µM general metalloproteinase inhibitor GM6001 significantly reduced mPS induced AP-TROP2 release. **(B)** Western blot analysis of cell lysates for TROP2 fragments (V5 antibody, reducing conditions). Metalloproteinase inhibitors prevented aMP fragment formation in cell lysates, with GI23 being less efficient. **(C&D)** mPS dependent AP-TROP2 release is not affected by blocking classical (1 µM Gö6979) or novel (1 µM Bim-1) PKCs using AP-activity assays. Western blot analysis confirms the presence of aMP fragments in mPS stimulated conditions regardless of classical or novel PKC inhibition. **(E&F)** Nanosight analysis of particle release into medium shows that mPS treatment caused a slight increase in particle numbers with which are approximately 20 nm smaller than control vesicles. The increase in vesicle numbers was not statistically significant.

**Figure 6: Inhibition of endocytosis with dynasore blocks mPS induced AP-TROP2 release and alternative cleavage and retains TROP2-ECD levels at the cell membrane**

**(A)** Inhibition of endocytosis with dynasore blocks mPS induced AP-TROP2 release into medium. **(B&C)** The average vesicle size in dynasore/mPS treated conditions is 107 nm while control vesicles are larger (127 nm). Dynasore blocks mPS dependent vesicle release. **(D&E)** Dynasore treatment ablates aMP fragment formation in lysates and in medium (right panel E). Note that under non-reducing conditions mPS induced AP-TROP2 release causes an increase in a band running at full length AP-TROP2 which is absent in mPS/dynasore co-treated samples (left panel E). **(F)** Confocal analysis of TROP2-ECD and TROP2–ICD domains using anti-TROP2 (green) and anti-V5 (red) antibodies shows good co-localisation for control and mPS treated cells. Dynasore treatment resulted in the loss of both TROP2 domains in the absence of mPS. In contrast mPS and dynasore treated samples retained cell surface localisation of TROP2-ECD and TROP2–ICD domains. Pearson's coefficient values were calculated as r=0.82, 0.84, 0.58 and 0.83 for each experimental condition. Bar is equivalent to 10 µm. **(G)** Fluorescence intensity analysis for TROP2-ECD and –ICD staining of the confocal experiment in **(F)**. In mPS and dynasore co-treated samples TROP2-ECD and –ICD staining is preserved.

**Figure 7: Schematic representation of TROP2 release leading to (A) ectosomal release and shedding of TROP2 or (B) alternative cleavage.**

**(A)** Activation of classical PKC activity leads to ectosomal TROP2 release that is blocked by Gö6979, while novel PKC activity activates TROP2 shedding by ADAM17 and TROP2-ECD monomer/dimer accumulation in medium. This was blocked by Bim-1 but not Gö6979.

**(B)** Inhibition of PKCζ using a myristoylated pseudopeptide substrate or shRNA knockdown causes initial TROP2 endocytosis and exosomal release of an alternatively cleaved TROP2, which remains membrane associated via a disulphide bridge. Gö6979 or Bim-1 treatment did not affect alternative cleavage, while ADAM10/17, ADAM10 or general metalloproteinase inhibitors prevented alternative cleavage. Inhibition with dynasore blocked exosomal release and alternative TROP2 cleavage.

Wanger et al. Fig. 1

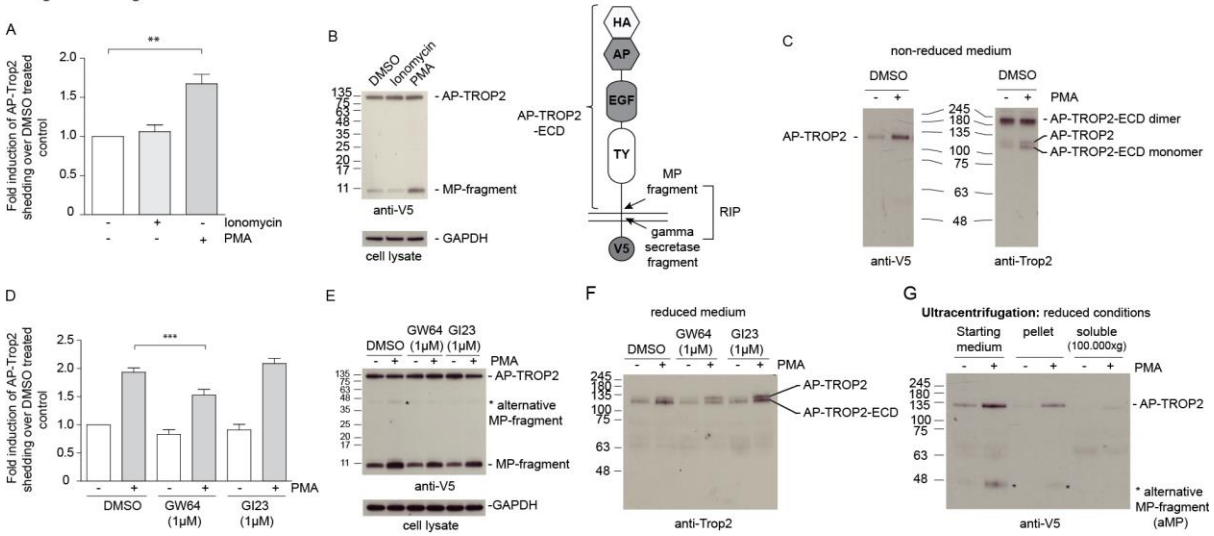

Wanger et al. Fig. 2

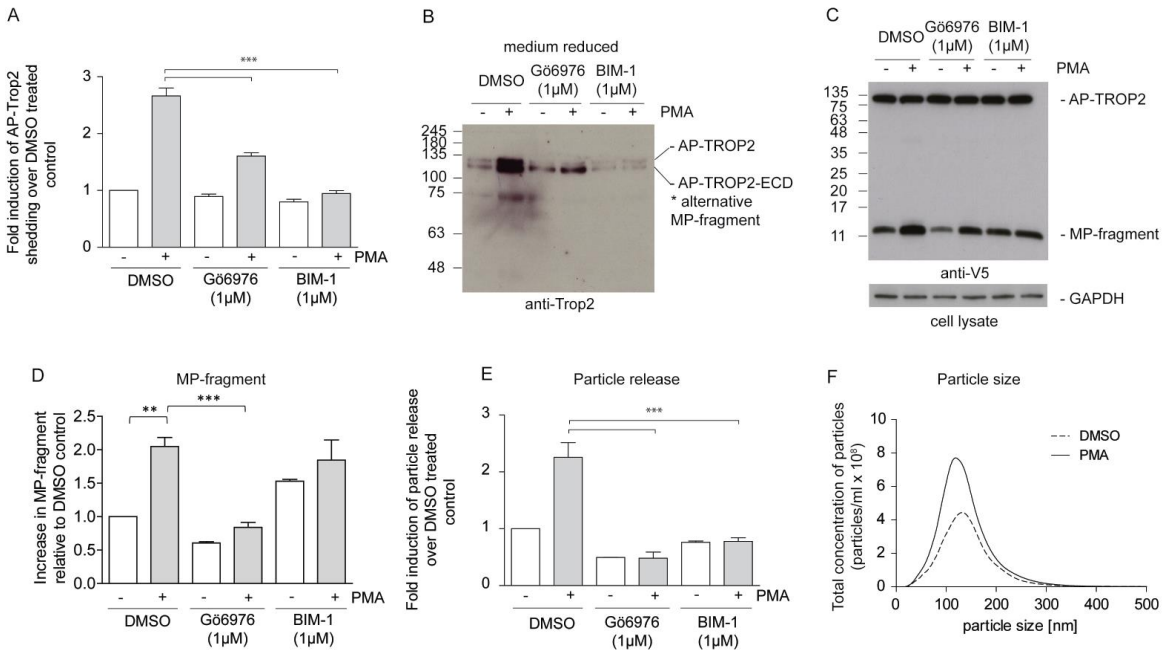

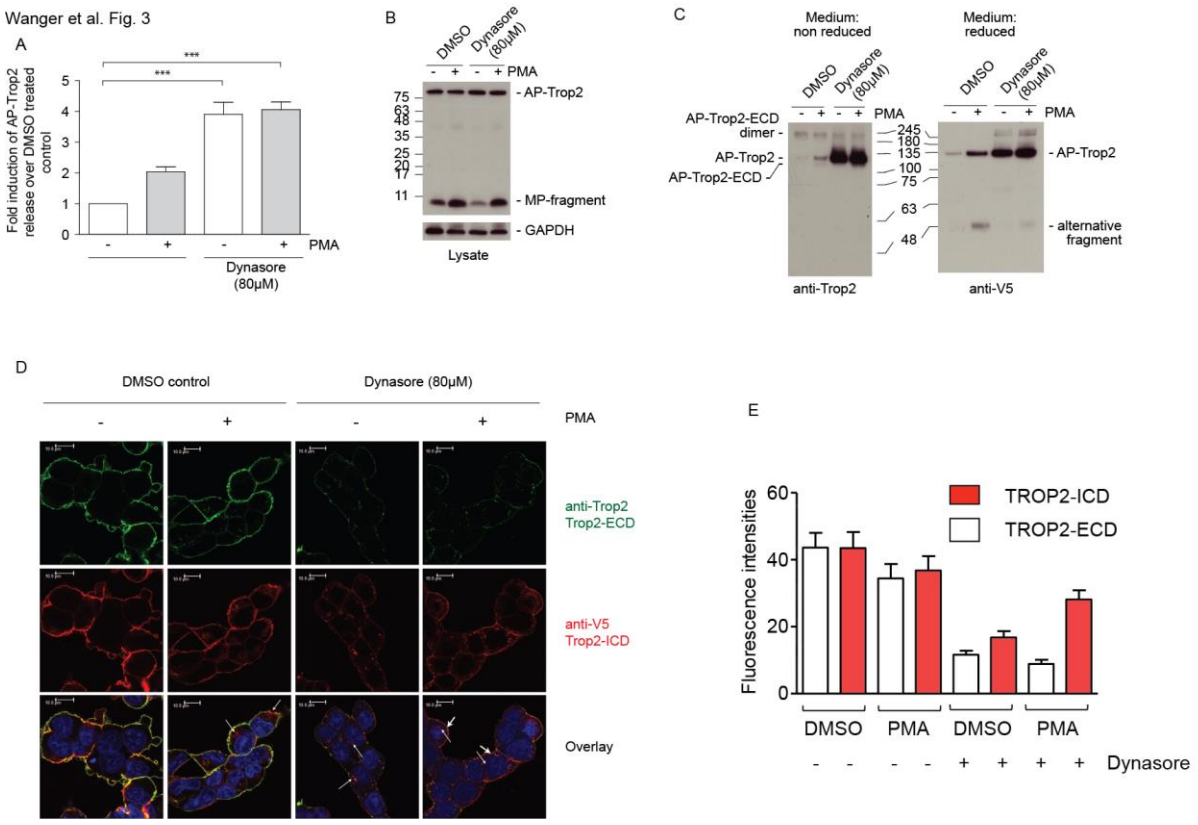
Wanger et al. Fig. 3
A
Fold induction of AP-Trop2 release over DMSO treated control
PMA
Dynasore (80µM)
B
DMSO
Dynasore (80µM)
PMA
- AP-Trop2
- MP-fragment
- GAPDH
Lysate
C
Medium: non reduced
Medium: reduced
AP-Trop2-ECD dimer
AP-Trop2
AP-Trop2-ECD
- alternative fragment
anti-Trop2
anti-V5
D
DMSO control
Dynasore (80µM)
anti-Trop2 Trop2-ECD
anti-V5 Trop2-ICD
Overlay
E
TROP2-ICD
TROP2-ECD
Fluorescence intensities
DMSO
PMA
Dynasore

Wanger et al. Fig. 4

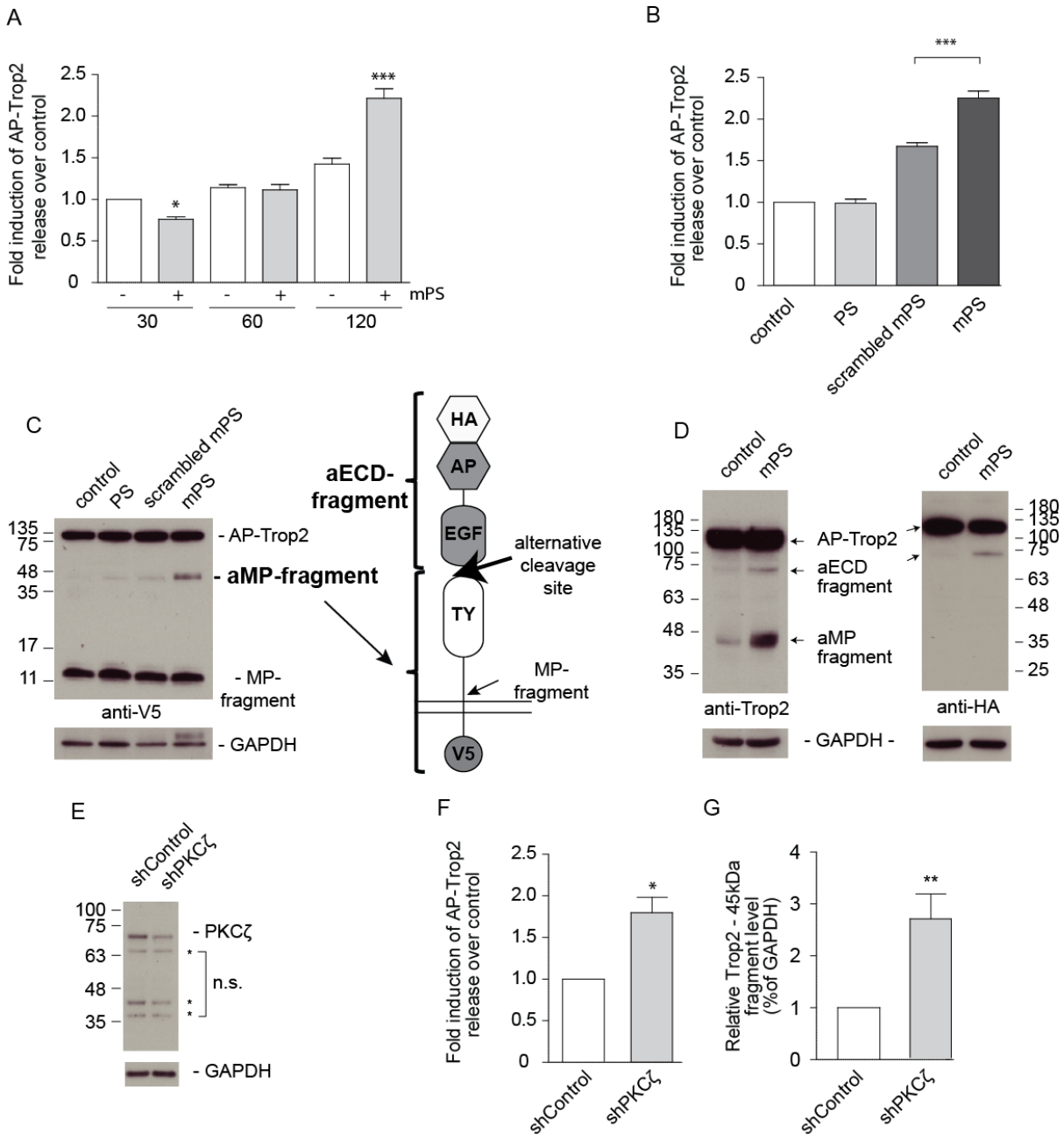

Wanger et al. Fig. 5

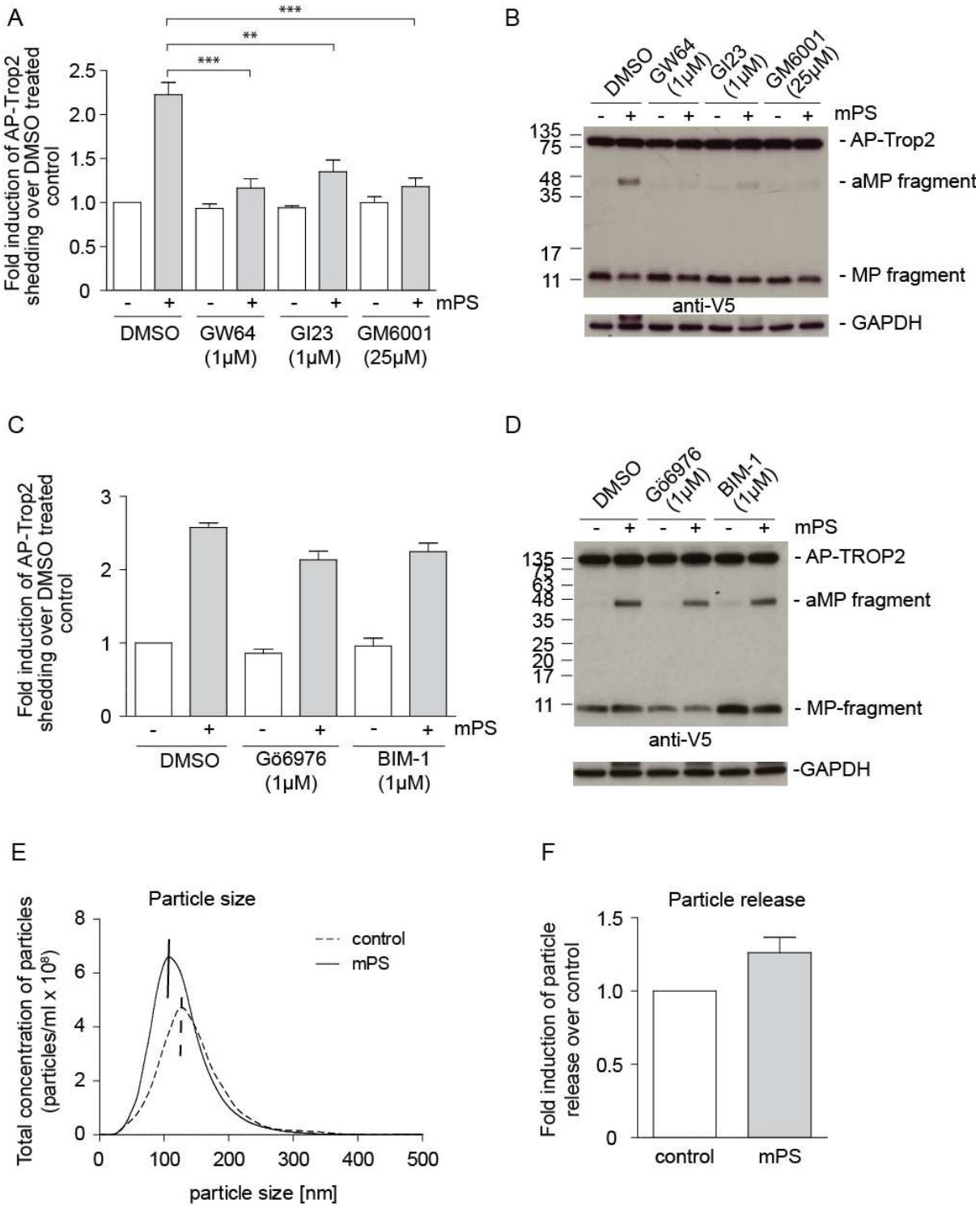

Wanger et al. Fig. 6

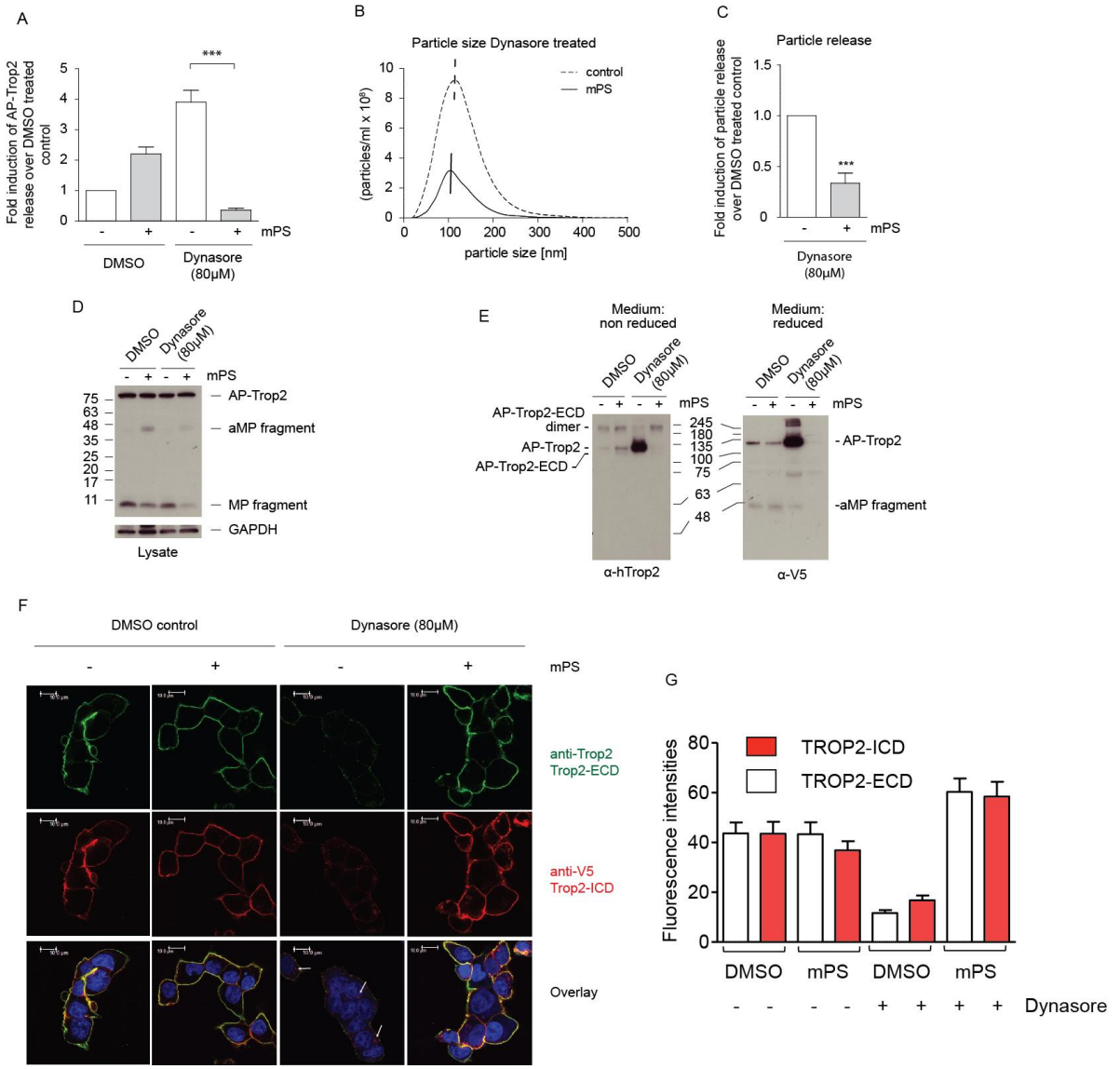

Wanger et al. Figure 7